

Impacts of subsidy policies on vaccination decisions in contact networksHai-Feng Zhang,^{1,2} Zhi-Xi Wu,³ Xiao-Ke Xu,⁴ Michael Small,⁵ Lin Wang,⁶ and Bing-Hong Wang⁷¹*School of Mathematical Science, Anhui University, Hefei 230039, China*²*Department of Electronic and Information Engineering, Hong Kong Polytechnic University, Hung Hom, Kowloon, Hong Kong, China*³*Institute of Computational Physics and Complex Systems, Lanzhou University, Lanzhou 730000, China*⁴*College of Information and Communication Engineering, Dalian Nationalities University, Dalian 116605, China*⁵*School of Mathematics and Statistics, University of Western Australia, Crawley, Australia*⁶*Adaptive Networks and Control Laboratory, Department of Electronic Engineering, Fudan University, Shanghai 200433, China*⁷*Department of Modern Physics, University of Science and Technology of China, Hefei 230026, China*

(Received 18 April 2013; published 18 July 2013)

To motivate more people to participate in vaccination campaigns, various subsidy policies are often supplied by government and the health sectors. However, these external incentives may also alter the vaccination decisions of the broader public, and hence the choice of incentive needs to be carefully considered. Since human behavior and the networking-constrained interactions among individuals significantly impact the evolution of an epidemic, here we consider the voluntary vaccination on human contact networks. To this end, two categories of typical subsidy policies are considered: (1) under the free subsidy policy, the total amount of subsidy is distributed to a certain fraction of individual and who are vaccinated without personal cost, and (2) under the partial-offset subsidy policy, each vaccinated person is offset by a certain amount of subsidy. A vaccination decision model based on evolutionary game theory is established to study the effects of these different subsidy policies on disease control. Simulations suggest that, because the partial-offset subsidy policy encourages more people to take vaccination, its performance is significantly better than that of the free subsidy policy. However, an interesting phenomenon emerges in the partial-offset scenario: with limited amount of total subsidy, a moderate subsidy rate for each vaccinated individual can guarantee the group-optimal vaccination, leading to the maximal social benefits, while such an optimal phenomenon is not evident for the free subsidy scenario.

DOI: [10.1103/PhysRevE.88.012813](https://doi.org/10.1103/PhysRevE.88.012813)

PACS number(s): 05.65.+b, 02.50.Le, 87.23.Ge, 89.75.Fb

I. INTRODUCTION

Preemptive vaccination is a fundamental method for preventing the transmission of infectious diseases as well as reducing morbidity and mortality [1]. Many well-studied strategies generally assume that vaccination or immunization can be compulsively enforced, such as via target immunization [2], ring vaccination [3], or acquaintance immunization [4]. For many nonlethal and vaccine-preventable diseases, e.g., measles, chickenpox, influenza, the voluntary vaccination strategy is usually adopted. If the choice of whether or not to vaccinate is determined by self-interest, the responses of human behavior to a disease will substantially impact the effectiveness of the vaccination program, which means that the disease-behavior feedback regulates the outcome of the control measures [5–8]. To characterize this decision-making process, game theory has been introduced into the epidemiological modeling framework, in which the vaccination behaviors of individuals depend on many socioeconomic factors such as the perceived risk of infection, the cost of vaccination, and the vaccination behavior of neighboring individuals [9–21]. For instance, Bauch *et al.* [9,10] analyzed the collective behavior of voluntary vaccination for various childhood diseases within a game-theoretic framework and found that this voluntary strategy cannot lead to the group-level optimum due to the risk perception pertaining to the vaccine and the effect of “herd immunity” (also known as the phenomenon of “externality” within the economics literature [22]). The imitation dynamics inherent in the strategy-updating process was considered in the game-based vaccination model in Ref. [11], where the oscillations of vaccine uptake can emerge under some specific

conditions, such as the change of disease prevalence or a high perceived risk of vaccine. In addition, Vardavas *et al.* [12,13,17] studied the effect of voluntary vaccination for influenza by using the minority game, by which the same theoretical framework successfully captured this scenario.

These seminal works mainly study the well-mixed population, where each individual has the same probability to contact others. In recent decades, the network-based epidemiology models have also attracted myriad attention [23–25]. Many works have studied epidemic spreading on human contact networks where nodes correspond to individuals and links reflect the contact between individuals by which the infection can be transmitted [26–33]. With respect to the well-mixed epidemics model, one of the most striking features of the network-based spreading model (without human behavior response) is the absence of epidemic threshold in the infinitely large and sufficiently heterogeneous networks [34–36]. As the topology of networks characterizes the contact structure among individuals to an extremely fine-grained level, much attention has been paid to investigate the interplay among contact patterns, behavioral responses, and disease dynamics by incorporating game theory, leading to many important results [37–39]. For example, Perisic *et al.* [37] reported that the voluntary vaccination can control a disease in low-degree networks, but as the average degree increases, the system will reach a critical threshold above which it behaves like a well-mixed population. Cornforth *et al.* [38] studied the voluntary vaccination behavior in different contact networks and discovered that a myopic vaccination decision can induce more serious oscillation of both vaccination coverage and epidemic size than what has been observed in reality. However,

such oscillations will become less variable when the number of prior seasons that individuals recall is increased. Fu *et al.* [39] demonstrated that degree heterogeneity of the network can also trigger a broad spectrum of individual vaccinating behavior. Naturally, “hubs” who have many neighbors are most likely to choose to be vaccinated, since they are at greatest risk of infection.

The impact of subsidy policies on controlling the epidemic spreading has been addressed in Refs. [40–44], which mainly consider the scenarios of well-mixed population from the socioeconomic perspectives. In this article, we will examine the effects of subsidy policies on the voluntary vaccination under the framework of network epidemiology, by which we expect to inspect whether the previous results obtained with the well-mixed population are still suitable to the networking scenarios. We also try to answer the following two questions: (1) How do people regulate their vaccination behaviors according to the decisions of neighboring individuals? and (2) How can we maximize the utility, given that the available subsidy is insufficient?

With the above arguments, in this work we develop a network-based vaccination model where individuals update their vaccination decisions by balancing the advantage and disadvantage of vaccination. We find that, due to the “herd immunity” effect of voluntary vaccination, diseases can rarely be eradicated. Hence, two categories of subsidy policies are considered: we first consider the free subsidy scenario, where a certain fraction of individuals are vaccinated without personal cost with the limited amount of subsidy; we also consider another scenario labeled the partial-offset subsidy policy, where a certain proportion of subsidy is distributed to *all* vaccinated persons. We find that the free subsidy policy is not helpful in improving the willingness of vaccination among nondonees, but rather actually reduces it. Therefore the free policy cannot yield expected results. In contrast, the partial-offset policy successfully encourages many more individuals to take vaccination, leading to the better performance with respect to the free subsidy policy when the same amount of subsidy is supplied. We further study the problem of how to produce the best results with a limited subsidy. For the partial-offset subsidy policy, the maximal population-level benefits as well as the lowest disease prevalence can be achieved if the limited subsidy is reasonably distributed. However, for the free subsidy policy, the optimal phenomenon is subtle or difficult to reach. Finally, to check the sensitivity of our results, we study our model under different conditions, such as the effectiveness of vaccines, the network structures, and so on, and we find that our results are robust under this sensitivity analysis.

II. THE MODEL

We study the impact of voluntary vaccination under these subsidy policies on the epidemic dynamics, with the underlying structure of human interactions represented by two kinds of typical complex networks. As the heterogeneous networks are often used to explore the spreading of epidemics, we first consider our dynamic process on the standard finite-size scale-free network: the Barabási-Albert preference attachment model with the average degree $\langle k \rangle = 6$ and the number of nodes $N = 2000$ (labeled BA network) [45]. To verify the

universality of our results, we also simulate the dynamic process on the Erdős-Rényi random graph with size $N = 2000$ and average degree $\langle k \rangle = 6$ (labeled the ER network) [46], as this interaction structure was considered in Refs. [37].

The dynamic process in our model is composed of two stages, i.e., the vaccination decision formation process and the epidemic process. In reality, before the deployment of vaccines, there is always a decision-making process that each individual can judge whether or not to vaccinate according to many factors, such as the self-interest. It is unusual for each individual to make their decision immediately before the arrival of vaccines, but they are often swayed by the tradeoff weighting. This evolutionary process can be characterized by a decision updating procedure [21,39], which proceeds with discrete time. After each individual makes his choice, the standard SIR (susceptible-infective-removed) epidemics dynamics is triggered by randomly chosen five unvaccinated individuals as the infectious seeds. Other individuals are either susceptible or vaccinated. In the following, we specify the mechanisms of the dynamic processes in more detail.

A. Vaccination decision formation process

The vaccination and the epidemic dynamics are implemented on human interaction networks. Initially, each individual is assigned a vaccination choice, i.e., to vaccinate or not, with an equal probability, such that the initial vaccination coverage on the network is about 50%. Then, we start the vaccination decision updating process, in which individuals need to decide whether or not to vaccinate before the final implementation of the vaccination program. According to many seminal works [9,10,21], each individual i 's vaccination decision is primarily influenced by self-interest, which relates to the perceived benefits of vaccination, P_i^v , and the perceived benefits of infection, P_i^n . By considering a nonlethal diseases, for simplicity, we assume that the vaccine is risk-free and provides full protection against infection. Thus the cost of vaccination, C_V , may correlate to the immediate expenditure, the time spent to get the vaccine, and other related health side-effects, e.g., fever, arm swelling, and nasal congestion [14]. We further define the cost of infection and the perceived probability of infections as C_I, λ_i for individual i . With these arguments, for each individual i , the payoff pertaining to the vaccination and infection can be summarized as

$$P_i^v = -C_V, \quad (1)$$

$$P_i^n = -C_I \lambda_i. \quad (2)$$

Without loss of generality, by letting $C_I = 1.0$ and $c = C_V/C_I$ (generally speaking, the vaccination cost should be lower relative to the cost of infection, and thus the relative cost of vaccination c is confined to the range $0 < c < 1$), then Eqs. (1) and (2) can be rewritten as

$$P_i^v = -c, \quad (3)$$

$$P_i^n = -\lambda_i. \quad (4)$$

According to Ref. [21], we define the perceived probability of infection λ_i as a function of the disease transmission rate β ($0 < \beta < 1$) and the number of unvaccinated neighbors k_{nv}^i :

$$\lambda_i = 1 - (1 - \beta)^{k_{nv}^i}. \quad (5)$$

Equation (5) implies that the greater the number of unvaccinated individuals among one's neighborhood, the higher the probability of infection.

At each time step, individuals update their vaccination decisions by maximizing the perceived benefits (in other words, by reducing their potential loss). In addition, as people are generally not perfect rational calculators, we also consider that the individuals have bounded rationality. This means that although individuals prefer to choose strategies with higher payoffs (payoff maximization rule), it is still possible for them to make errors that lead to the choice of low payoff decision. The standard way to realize this objective is to incorporate a stochastic element into the decision updating process. By using the Fermi function that is widely used in the studies of evolutionary game theory [21,47–50], the probability of choosing to vaccinate for any individual i is defined as

$$P_i = \frac{1}{1 + e^{-\alpha(P_i^v - P_i^n)}}, \quad (6)$$

where the parameter $\alpha (\geq 0)$ governs the selection strength reflecting the responsiveness of individuals to the difference of payoffs. $\alpha = 0$ means totally random selection, while $\alpha = \infty$ corresponds to the local best-response selection. Without any special statement, we set $\alpha = 5$ in this paper, which implies that the better strategy is readily adopted, yet it is not impossible that individuals will occasionally select a worse strategy. Moreover, $\alpha = 5$ is large enough to bring the irrational element into the decision-making process, but not too small to overshadow the effect of best response based on the payoff maximization.

This vaccination decision-making process is carried out in parallel until reaching some steady state. At this stage, the last 100 iterations of the total 1000 steps are used in our model, which is sufficiently long [21].

B. Epidemic dynamics

For the epidemics dynamics, we consider the usual SIR compartmental model. At each time step, susceptible individual i will be infected with the probability $\Lambda_i = 1 - (1 - \beta)^{k_{inf}^i}$, where k_{inf}^i is the number of infected neighbors of i . Any

infectious individual recovers and become immune with the rate μ per unit time. We run the dynamic process with the Monte Carlo simulations, until no infectious individuals remain in the system. In this paper, without any special statement, we assume the transmission rate $\beta = 0.18 \text{ d}^{-1} \text{ person}^{-1}$ and the recovery rate $\mu = 0.25 \text{ d}^{-1}$ [20,39], which ensures that with an initial entire unvaccinated population the average final epidemic size (the final fraction of infected individuals) is approximately equal to 90% [21,39].

The simulation result for each set of parameters is obtained by averaging over 100 independent runs of the entire dynamics process. In each holistic realization of the dynamic process, the final epidemic size is obtained by averaging over 20 random runs of the epidemic process.

III. EFFECTS OF SUBSIDY POLICIES

We first report the results with the free subsidy policy in Fig. 1. In this scenario, the total amount of subsidy (labeled S) is distributed to a certain fraction of individuals, and all donees are vaccinated without personal cost. For instance, given the total amount of subsidy $S = 100$ and $c = 0.5$, 200 persons will participate in vaccination without personal cost. In Fig. 1, we also present the scenario of $S = 0$ as the baseline that excludes the stressed external policy, in which the vaccination coverage (V) among the entire population decreases rapidly with the increase of c [see Fig. 1(b)], leading to the rise of final epidemic size [I ; see Fig. 1(a)]. When the free subsidy policy is introduced into the model, as shown in Fig. 1, one can find that the effect of intervention is not very remarkable (with respect to that of the partial-offset policy discussed in the following), especially when c is large. Although the value of S has been increased from 0 to 400, there is only a limited effect on reducing the final epidemic size [see Fig. 1(a)].

To better understand this unsatisfactory situation, we report the vaccination coverage among nondonees (V_{nd}) in Fig. 1(c). The values of V_{nd} under the free subsidy policy ($S > 0$) are lower than that of the baseline ($S = 0$). According to Eq. (6), the perceived infection risk of those nondonees will reduce if more individuals are vaccinated with subsidy, leading to the

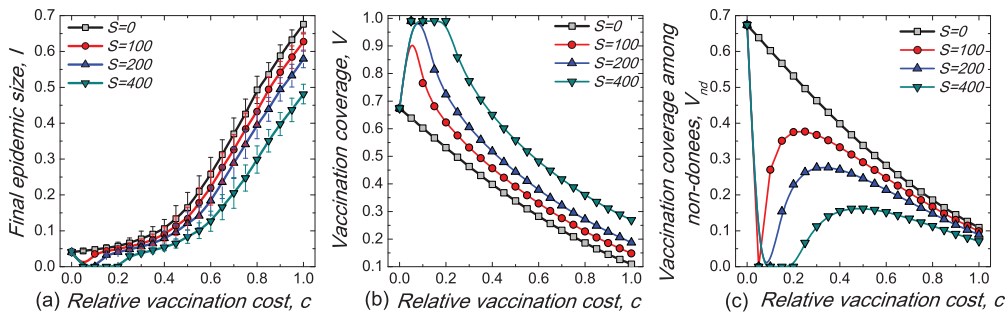


FIG. 1. (Color online) The impact of free subsidy policy on the vaccination behaviors and the final epidemic size with several typical values of the total amount of subsidy S . We present the final epidemic size (a), the vaccination coverage among the entire population (b), and the vaccination coverage among nondonees (c) as functions of the relative cost of vaccination c . It is worth mentioning that with a very small value of c and large value of S , e.g., $c = 0.05, S = 200$, the number of donees will be larger than the population size, i.e., $S/c > N = 2000$. In this case, all individuals will be vaccinated without personal cost. We also limit $S = 0$ when $c = 0$. The average value and the standard deviation (error bar) are shown for each set of parameters in panel (a). In panels (b) and (c), the error bar is not shown as the standard deviation is much small (less than 10^{-1} of the average value).

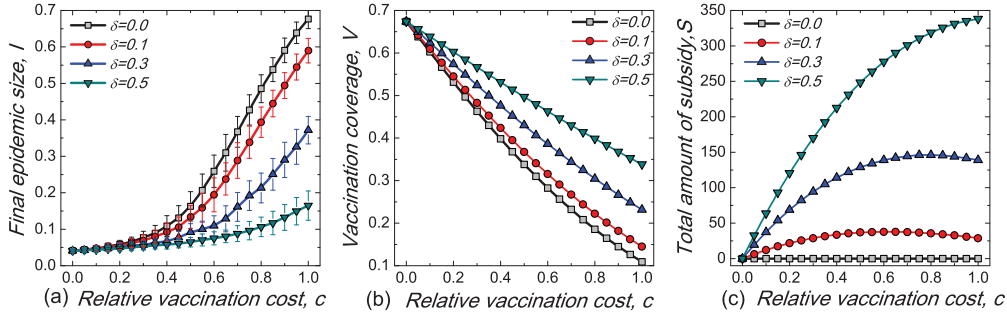


FIG. 2. (Color online) The impact of partial-offset subsidy policy on the vaccination behavior and the final epidemic size with several typical values of δ , i.e., $\delta = 0.1, 0.3, 0.5$. The scenario of $\delta = 0$ is considered as the baseline excluding the subsidy policy. We show the final epidemic size (a), the vaccination coverage over the entire population (b), and the total amount of subsidy as functions of the relative cost of vaccination c .

fact that nondonees are more prone to take risks after balancing the advantage and disadvantage of vaccination.

Under the partial-offset subsidy policy, the vaccination cost for each individual is reduced to $(1 - \delta)c$, which means that a proportion δc of cost for each vaccinated individual will be covered by the subsidy policy. The effect of partial-offset policy on the epidemic evolution is presented in Fig. 2. As shown in Fig. 2(b), with the increase of δ , the vaccination coverage among the entire population is also monotonically elevated, leading to a sharp decline for the final epidemic size, which is more notable than what we can expect for the free policy. For example, when $c = 1.0$, the final epidemic size is cut down from about 0.65 to 0.15 as δ increases from 0 to 0.5. More significantly, this strategy requires a smaller total amount of subsidy, S , with respect to the free subsidy scenarios. For instance, even 50% of the vaccination cost is covered by the partial-offset policy, i.e., $\delta = 0.5$, the total amount of subsidy S is still smaller than 350 [Fig. 2(c)], whereas the performance of this case in decreasing the final epidemic size is much better than that of the free subsidy scenario with $S = 400$ [see Fig. 1(a) and Fig. 2(a)]. The advantage of the partial-offset policy lies in the fact that: for each vaccinated individual, the cost of vaccination is reduced due to the endowment of the policy.

We next compare the effects of these two subsidy policies with the same total subsidy S in Fig. 3. Note that under the partial-offset policy, the total subsidy S is not predetermined, but depends on the number of vaccinated individuals, the value of δ , and the relative cost of vaccination c . To fairly compare the two subsidy policies, the following procedure is adopted: We first measure the total subsidy S for each c under the partial-offset policy, by fixing the value of δ , by which we use the same values of S and c to the free policy. Therefore, the final epidemic sizes of these two subsidy policies can be acquired with the same S , by which we compare the difference of final epidemic size between the free policy (I_f) and the partial-offset policy (I_p). As shown in Fig. 3, the final epidemic size under the free policy is larger than that of the scenario of partial-offset policy. Moreover, we can find that the advantage of the partial-offset policy becomes more and more pronounced with the increase of c .

From the perspective of group interest, the purpose of introducing subsidy policies is to minimize the total social cost at the entire population level or to cut down the number of

infected individuals. Often in reality, the available budget for supplying the subsidy is limited. Therefore, it is important to design an optimal subsidy strategy for maximizing the utility of this limited resource. We first consider the situation that the optimal objective is to minimize the total social cost at the population level. By combining Eqs. (3) and (4), the total social cost SC is defined as [10,51]

$$SC = N_R \times 1.0 + N_V \times c, \quad (7)$$

where N_R, N_V denote the final number of infected (also recovered) and vaccinated individuals. Figure 4(a) shows the phase diagram of the social cost SC dependent on the vaccination cost c and the total amount of subsidy S , under the free subsidy policy. The parameter space is divided into three separate regions. In the left-bottom region 1 (the parameter space between the red solid line and the purple dashed line), with each given c , the total social cost SC increases with the augment of S . This implies that further increasing the subsidy is unnecessary in this case. In the upper-left region 2 (on the left of purple dashed line), as $S/c > N$, all individuals are vaccinated without personal cost. In the region 3 (on the right of the red solid line), one can find that with each given c there presents a subtle optimal value of S leading to the

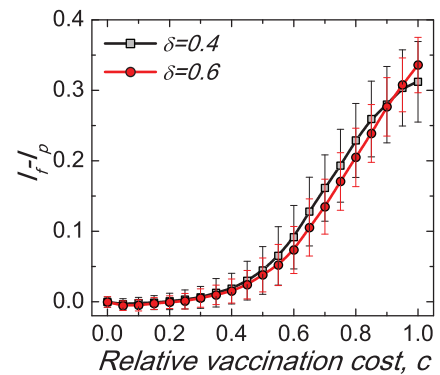


FIG. 3. (Color online) The comparison of the final epidemic size between the free subsidy and partial-offset scenarios with two typical values of δ . Each data point is obtained with the condition that the same amount of total subsidy is supplied to each case. I_f, I_p denotes the final epidemic size under the free subsidy and partial-offset policies, respectively. With the increase of the relative vaccination cost, c , the difference between I_f and I_p continues to increase.

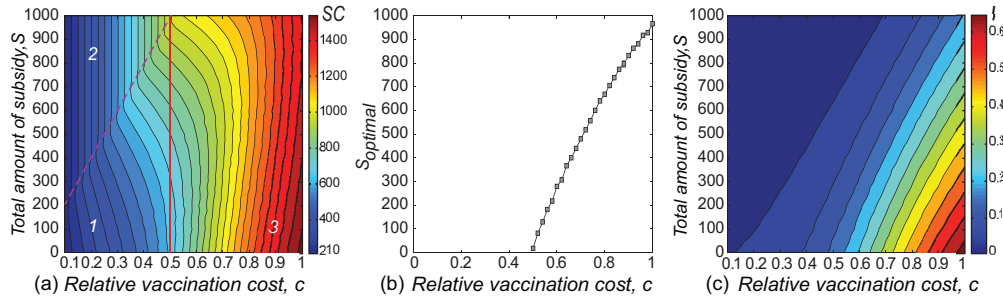


FIG. 4. (Color online) The phase diagrams of the social cost SC (a) and the final epidemic size I (c) under the free subsidy policy. The inspected parameters are the relative cost of vaccination c and the total amount of subsidy S . In panel (a), there are three different phase regions, separated by the red solid line and the purple dashed line. When the total subsidy amount S reaches the maximum value (i.e., $S = 1000$ here), all individuals can be vaccinated without personal cost when $c \leq 0.5$, while when $c > 0.5$ only a fraction of the population can be freely vaccinated even with this high S . Thus the red solid line identifies this crossover. The purple dashed line is used to characterize the relation $S = cN$. In region 2 above the purple dashed line, all individuals can be vaccinated without personal cost. Panel (b) reports the relation between the vaccination cost c and the optimal value S_{optimal} in the region 3 of panel (a). There is no line for $c < 0.5$ because of the absence of the optimal phenomenon in (a).

lowest level of the total social cost SC [also see Fig. 4(b)]. To quantify the effect of free policy on decreasing the number of infected individuals, we also report the phase diagram of the final epidemic size I in dependence on c and S . As shown in Fig. 4(c), one can clearly find that I increases with the augment of c , but decreases with the enhancement of S .

Under the partial-offset subsidy policy, the total amount of subsidy S is determined by the parameters c, δ , but cannot be predetermined. Hence we focus on studying the impact of these two parameters on the total social cost SC . As shown in Fig. 5(a), the specific values of δ do not have a significant influence on the social cost SC when the relative vaccination cost c is small (see the region on the left of the red solid line). This is mainly because individuals are likely to take vaccination by themselves when c is small, thus the subsidy policy is unnecessary. With a large value of c (the region on the right of the red solid line), one can find that there is always an optimal value of δ for each c , leading to the minimum of total

social cost SC . As shown in Fig. 5(b), the optimal value δ_{optimal} increases monotonically with c , which means that the higher the relative vaccination cost c is, the larger the proportion of the cost should be covered by the subsidy. It is worth stressing that with very large value of c ($c \sim 1$), δ_{optimal} is neither 0 nor 1. In other words, the best cost-effective partial-offset strategy cannot be achieved by either entirely free vaccination without personal expenditure or costly vaccination covering all individuals.

We next quantify the effect of partial-offset policy on reducing the number of infected individuals. We here append a constraint by limiting the total amount of available subsidy S . This consideration is more close to the real situation and provides more information on designing the most cost-effective subsidy policy. As shown in Fig. 6, where S increases from 100 to 600 in panels (a)–(f), it is clear that for each given S there presents an optimal δ leading to the smallest

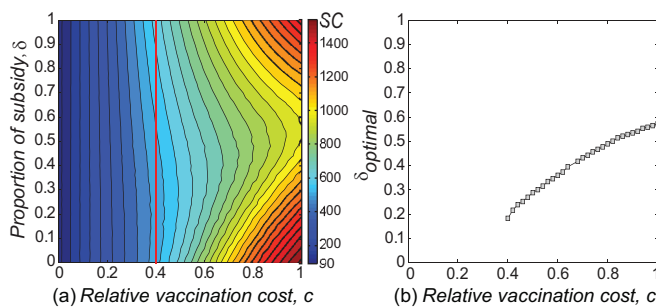


FIG. 5. (Color online) The phase diagram of the social cost SC under the partial-offset policy as a function of the relative vaccination cost c and the subsidy proportion δ . In panel (a), the region on the left of the red solid line reflects that the effect of the strategy is negligible when c is small, while in the right part of this panel there always presents an optimal value of δ inducing the minimal SC for each c . Panel (b) reports the corresponding relation between the relative vaccination cost c and the optimal value δ_{optimal} in this right region of panel (a). There is no line for $c < 0.4$ because of the absence of the optimal phenomenon in (a).

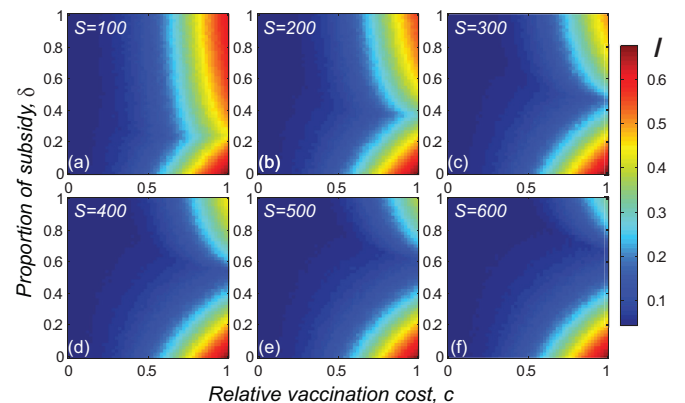


FIG. 6. (Color online) The phase diagrams of the final epidemic size I as a function of the relative vaccination cost c and the proportion of subsidy δ , with limited amount of total subsidy. Six typical values of total subsidy S are considered, i.e., $S = 100, 200, 300, 400, 500, 600$. It is worth mentioning that, with given S , if $\delta c N_V < S$, the actual used amount of subsidy $S = \delta c N_V$. In each panel, there is an optimal value of δ leading to the least final epidemic size when c is not small. As S increases the optimal value of δ also becomes larger.

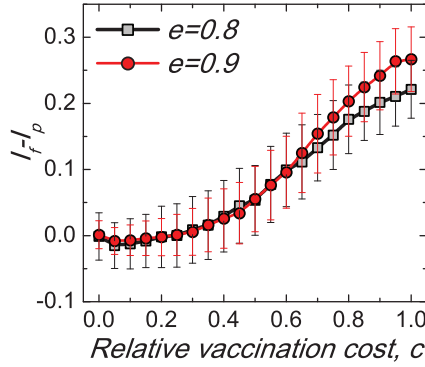


FIG. 7. (Color online) The comparison of the final epidemic size between the free subsidy and partial-offset scenarios, by considering two typical effective rate e of the vaccine. Each data point is obtained with the condition that the same amount of total subsidy is supplied to each case. We fix $\delta = 0.4, \alpha = 5.0$. The approach for producing this figure is similar to what we used in Fig. 3.

final epidemic size when the relative vaccination cost c is large. Interestingly, the optimal value of δ increases with S . This can be explained from two aspects. When each vaccinated individual only receives very limited support from the subsidy policy, which corresponds to a small value of δ , much of the supplied subsidy cannot be completely exhausted ($\delta c N_V < S$). In this case, the utility of this subsidy policy has been underestimated and wasted. When a large proportion from the expenditure of each vaccinated individual can be covered by the subsidy policy, which means δ is very large, only a few individuals have the chance to receive this valuable incentive. This is similar to the scenario of free subsidy policy. In this case, the partial-offset policy fails to encourage considerable individuals to take vaccination. Therefore, given the total subsidy is limited, the most efficient strategy is to assist each vaccinated individual with an intermediate level of subsidy, which can promote more people to participate in the vaccination.

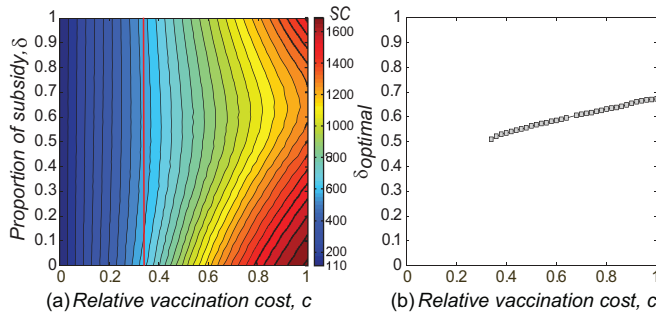


FIG. 8. (Color online) Sensitivity analysis of the optimal phenomenon on the ER network with $N = 2000, \langle k \rangle = 6$, and the transmission rate $\beta = 0.155 \text{ d}^{-1} \text{ person}^{-1}$. Other parameters are similar to Fig. 5. (a) The region on the left of the red solid line reflects that the effect of the strategy is negligible when c is small, while in the right part of this panel there always presents an optimal value of δ resulting in the minimal SC for each c . (b) The relation between the relative vaccination cost c and the optimal value δ_{optimal} in the right region of panel (a). There is no line for $c < 0.34$ because of the absence of the optimal phenomenon in (a).

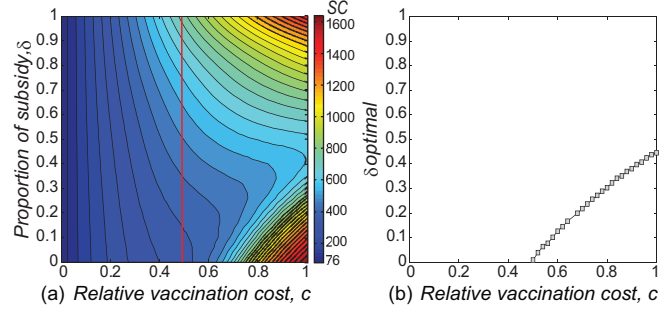


FIG. 9. (Color online) Sensitivity analysis of the optimal phenomenon with the selection strength $\alpha = 15$. Other parameters are similar to what was used in Fig. 5. (a) The region on the left of the red solid line still reflects that the effect of the considered strategy is negligible when c is small, while in the right part of the panel there always emerges an optimal value of δ corresponding to the minimal SC for each c . (b) The relation between the relative vaccination cost c and the optimal value δ_{optimal} in the right region of panel (a). There is no line for $c < 0.5$ because of the absence of the optimal phenomenon in (a).

Finally, we perform some sensitivity analysis to test the robustness of our results. We first consider the flawed vaccine scenario, where the effectiveness of the vaccine is smaller than 100%. As shown in Fig. 7, fixing $\delta = 0.4$, we compare the effects of the subsidy policies on reducing the final epidemic size I , as what we performed in Fig. 3. One can clearly find that, when the value of c is large enough ($c \geq 0.3$) the partial-offset policy still performs better than the counterpart strategy.

We also check the optimal phenomenon (see Fig. 5) with another kind of the network structure and different levels of strength of selection. Figure 8 shows the optimal results on the ER network, while Fig. 9 presents the optimal phenomenon with $\alpha = 15$. One can find clearly that the optimal δ still emerges under these two cases, when the relative vaccination cost is large enough.

IV. CONCLUSIONS

Incorporating the element of human behavioral response into the epidemics dynamics is important to enhance the applicability of epidemiology models. Towards this objective, the game-based voluntary vaccination provides a promising framework to better understand the complex interplay between human behavior and epidemic spreading. Besides this well-studied disease-behavior feedback phenomenon, in reality, various subsidy policies are also often supplied to encourage more people to participate in the vaccination campaign. In this work, we mainly study the effects of subsidy policies with network-based epidemiology modeling. Two categories of typical subsidy policies are considered, namely, the free subsidy policy and the partial-offset subsidy policy. Their impacts on the vaccination coverage and the final epidemic size have been systematically studied with extensive computer simulations. Without any external promotion, we find that the disease can hardly be controlled in the contact networks. The situation has not been meliorated remarkably under the free subsidy policy, because many nondonees cannot be encouraged sufficiently to take vaccination due to the presence

of “herd immunity” effect. In contrast, the effect of partial-offset subsidy policy is prominent, which effectively promotes the vaccination coverage. We also inspect their influence on the total social cost as well as the final epidemic size. Interestingly, under the partial-offset subsidy policy, a moderate subsidy rate for each vaccinated individual, δ , can guarantee the optimal cost effectiveness, whereas this phenomenon is not notable under the free subsidy policy.

Our study implies that optimization of the subsidy policies is indeed a sophisticated but critical problem. When designing certain regulatory measures, health sectors may need to carefully consider the potential human response to their

policies. Otherwise, it may be unable to achieve the expected objectives or generate unnecessary waste.

ACKNOWLEDGMENTS

This research was funded in part by the NSFC (Grants No. 11005001, No. 11005051, No. 61004104, No. 61104143, and No. 61004101), H.-F.Z. acknowledges support by the Doctoral Research Foundation of Anhui University (Grant No. 02303319). L.W. also acknowledges partial support by the Fudan University Excellent Doctoral Research Program (985 Project). M.S. is supported by an Australian Research Council Future Fellowship (FT110100896).

-
- [1] R. M. Anderson and R. M. May, *Infectious Diseases of Humans: Dynamics and Control* (Oxford University Press, Oxford, 1991).
- [2] R. Pastor-Satorras and A. Vespignani, *Phys. Rev. E* **65**, 036104 (2002).
- [3] J. Müller, B. Schönfisch, and M. Kirkilionis, *J. Math. Biol.* **41**, 143 (2000).
- [4] R. Cohen, S. Havlin, and D. ben-Avraham, *Phys. Rev. Lett.* **91**, 247901 (2003).
- [5] N. Ferguson, *Nature (London)* **446**, 733 (2007).
- [6] S. Lee, L. E. C. Rocha, F. Liljeros, and P. Holme, *PLoS ONE* **7**, e36439 (2012).
- [7] T. Gross and H. Sayama (eds.), *Adaptive Networks: Theory, Models and Applications* (Springer, Cambridge, MA, 2009).
- [8] L. B. Shaw and I. B. Schwartz, *Phys. Rev. E* **81**, 046120 (2010).
- [9] C. T. Bauch, A. P. Galvani, and D. J. D. Earn, *Proc. Natl. Acad. Sci. USA* **100**, 10564 (2003).
- [10] C. T. Bauch and D. J. D. Earn, *Proc. Natl. Acad. Sci. USA* **101**, 13391 (2004).
- [11] C. T. Bauch, *Proc. Roy. Soc. B: Biol. Sci.* **272**, 1669 (2005).
- [12] R. Vardavas, R. Breban, and S. Blower, *PLoS Comput. Biol.* **3**, e85 (2007).
- [13] R. Breban, R. Vardavas, and S. Blower, *Phys. Rev. E* **76**, 031127 (2007).
- [14] A. P. Galvani, T. C. Reluga, and G. Chapman, *Proc. Natl. Acad. Sci. USA* **104**, 5692 (2007).
- [15] S. Bhattacharyya and C. T. Bauch, *J. Theor. Biol.* **267**, 276 (2010).
- [16] H. F. Zhang, J. Zhang, C. S. Zhou, M. Small, and B. H. Wang, *New J. Phys.* **12**, 023015 (2010).
- [17] R. Breban, *PLoS ONE* **6**, e28300 (2011).
- [18] T. C. Reluga and A. P. Galvani, *Math. Biosci.* **230**, 67 (2011).
- [19] E. Shim, J. J. Grefenstette, S. M. Albert, B. E. Cakouros, and D. S. Burke, *J. Theor. Biol.* **295**, 194 (2012).
- [20] X. T. Liu, Z. X. Wu, and L. Zhang, *Phys. Rev. E* **86**, 051132 (2012).
- [21] M. L. Ndeffo Mbah, J. Z. Liu, C. T. Bauch, Y. I. Tekel, J. Medlock, L. A. Meyers, and A. P. Galvani, *PLoS Comput. Biol.* **8**, e1002469 (2012).
- [22] S. E. Holtermann, *Economica* **39**, 78 (1972).
- [23] M. E. J. Newman, *SIAM Rev.* **45**, 167 (2003)
- [24] M. J. Keeling and K. T. D. Eames, *J. Roy. Soc. Interface* **2**, 295 (2005).
- [25] S. Boccaletti, V. Latora, Y. Moreno, M. Chavez, and D. U. Hwang, *Phys. Rep.* **424**, 175 (2006).
- [26] L. A. Meyers, B. Pourbohloul, M. E. J. Newman, D. M. Skowronski, and R. C. Brunham, *J. Theor. Biol.* **232**, 71 (2005).
- [27] X. Li and X. F. Wang, *IEEE Trans. Auto. Control* **51**, 534 (2006).
- [28] M. Small, D. M. Walker, and C. K. Tse, *Phys. Rev. Lett.* **99**, 188702 (2007).
- [29] S. Meloni, A. Arenas, and Y. Moreno, *Proc. Natl. Acad. Sci. USA* **106**, 16897 (2009).
- [30] L. Wang, X. Li, Y. Q. Zhang, Y. Zhang, and K. Zhang, *PLoS ONE* **6**, e21197 (2011).
- [31] Q. C. Wu, X. C. Fu, M. Small, and X. J. Xu, *Chaos* **22**, 013101 (2012).
- [32] L. Wang, Y. Zhang, T. Huang, and X. Li, *Phys. Rev. E* **86**, 032901 (2012).
- [33] P. P. Shu, M. Tang, K. Gong, and Y. Liu, *Chaos* **22**, 043124 (2012).
- [34] R. Pastor-Satorras and A. Vespignani, *Phys. Rev. Lett.* **86**, 3200 (2001).
- [35] R. Parshani, S. Carmi, and S. Havlin, *Phys. Rev. Lett.* **104**, 258701 (2010).
- [36] C. Castellano and R. Pastor-Satorras, *Phys. Rev. Lett.* **105**, 218701 (2010).
- [37] A. Perisic and C. T. Bauch, *PLoS Comput. Biol.* **5**, e1000280 (2009).
- [38] D. Cornforth, T. C. Reluga, E. Shim, C. T. Bauch, A. P. Galvani, and L. A. N. Meyers, *PLoS Comput. Biol.* **7**, e1001062 (2011).
- [39] F. Fu, D. Rosenbloom, L. Wang, and M. Nowak, *Proc. Roy. Soc. B: Biol. Sci.* **278**, 42 (2011).
- [40] P. Geoffard and T. Philipson, *Am. Econ. Rev.* **87**, 222 (1997).
- [41] T. Philipson, in *Handbook of Health Economics*, edited by A. J. Culyer and J. P. Newhouse (North-Holland, Amsterdam, 2000), Vol. 1, p. 1761.
- [42] M. Gersovitz and J. Hammer, *J. Pub. Econ.* **89**, 647 (2005).
- [43] M. Gersovitz and J. Hammer, *World Bank Research Observer* **18**, 129 (2003).
- [44] S. Barrett and M. Hoel, *Environ. Dev. Econ.* **12**, 627 (2007).
- [45] A.-L. Barabási and R. Albert, *Science* **286**, 509 (1999).

- [46] P. Erdős and A. Rényi, *Publ. Math. Inst. Hung. Acad. Sci.* **5**, 17 (1960).
- [47] G. Szabó and C. Tóke, *Phys. Rev. E* **58**, 69 (1998).
- [48] H. F. Zhang, R. R. Liu, Z. Wang, H. X. Yang, and B. H. Wang, *Europhys. Lett.* **94**, 18006 (2011).
- [49] Z. Wang, L. Wang, Z. Y. Yin, and C. Y. Xia, *PLoS ONE* **7**, e40218 (2012).
- [50] A. Szolnoki, Z. Wang, and M. Perc, *Sci. Rep.* **2**, 576 (2012).
- [51] B. Dybiec, A. Kleczkowski, and C. A. Gilligan, *Phys. Rev. E* **70**, 066145 (2004).